Journal of Colloid and Interface Science 594 (2021) 47–53

Contents lists available at ScienceDirect

Journal of Colloid and Interface Science

journal homepage: www.elsevier.com/locate/jcis

Regular Article

Impact of residual gas on the optoelectronic properties of Cs-sensitized $In_{0.53}Ga_{0.47}As$ (001) surface

Qianglong Fang [a], Yang Shen [a,b,c,*], Shuqin Zhang [a], Xiaodong Yang [d,**], Lingze Duan [e], Liang Chen [a,**], Shiqing Xu [a], Mingxia Gao [b], Hongge Pan [b]

[a] Institute of Optoelectronics Technology, China Jiliang University, Hangzhou 310018, China
[b] School of Materials Science and Engineering, Zhejiang University, Zhejiang 310027, China
[c] Hengdian Group Tospo Lighting Co., Ltd., Dongyang 310007, China
[d] Key Laboratory of Ecophysics and Department of Physics, Shihezi University, Xinjiang 832003, China
[e] Department of Physics, The University of Alabama in Huntsville, Huntsville, AL 35899, USA

GRAPHICAL ABSTRACT

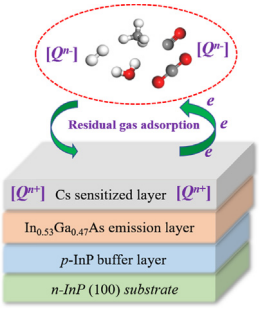

ARTICLE INFO

Article history:
Received 4 January 2021
Revised 7 March 2021
Accepted 8 March 2021
Available online 15 March 2021

Keywords:
$In_{0.53}Ga_{0.47}As$ surface
First-principles calculation
Residual gas
Dipole moments
Optical properties

ABSTRACT

Near-infrared $In_xGa_{1-x}As$ photocathode with better optoelectronic properties is a good candidate for low-light-level (LLL) night-vision system. However, the residual gases in the ultra-high vacuum (UHV) system inevitably affects the stability and photo-emission performance of LLL photoelectric devices such as their quantum efficiency and life-time. In this study, the first-principles calculations were used to investigate the adsorption effect of five different residual gas species, including H_2, CH_4, CO, H_2O and CO_2 on Cs-sensitized $In_{0.53}Ga_{0.47}As$ (001) β_2 (2 × 4) surface. The study results indicate that CO_2 gas molecule is the most easily attached to the Cs-sensitized surface. The adsorption of residual gases leads to the formation of a new dipole pointing from inner Cs atoms to gas molecules. It makes the charge center of the adsorbates escape from the surface, which weakens the interaction between the inner Cs atoms and the clean surface. This results in the increase of the surface work function and degradation of the performance of photoelectric devices. Also, the adsorption of residual gas molecules influences the absorption and reflection coefficients of Cs-sensitized $In_{0.53}Ga_{0.47}As$ (001) β_2 (2 × 4) surface.

1. Introduction

III-V semiconductors GaAs, InAs and their ternary mixed crystal InGaAs have attracted notable attention because they have potential electronic and optoelectronic applications. Also, due to their

* Corresponding author at: Institute of Optoelectronics Technology, China Jiliang University, Hangzhou 310018, China.
** Corresponding authors.
E-mail addresses: yshen1016@foxmail.com (Y. Shen), yxd1209@shzu.edu.cn (X. Yang), lchen@cjlu.edu.cn (L. Chen).

https://doi.org/10.1016/j.jcis.2021.03.043
0021-9797/

high-temperature stability, low ionicity, and other advantages [1,2], they have are prevalent in various photovoltaic devices, such as quantum dot lasers [3], solar cells [4], field-effect transistors [5]. In particular, alloy compounds based on InGaAs materials have higher electron transmission properties than GaAs, which makes them useful in the field of infrared light-emitting diode (LED) detections [6]. Moreover, surface activation can be achieved by depositing Cs and oxidant (O or NF_3) on the surface of semiconductor-based photocathode in ultra-high vacuum (UHV) environment. This leads to the state of negative electron affinity (NEA) [7,8]. In parallel, the surface activated through the adsorption of Cs atoms is also called Cs-sensitized surface [9]. Owing to its adjustable spectral response wavelength, NEA $In_xGa_{1-x}As$ photocathode has been considered to be a promising and powerful candidate for the preparation of near-infrared image-enhancement devices [10–12]. However, the short lifetime of NEA $In_xGa_{1-x}As$ photocathodes has always been the main limitation for their wide use [13,14]. Although much effort has been devoted to avoiding the high-power laser irradiation in the activation process, the quantum efficiency always decreases [15,16]. The compelling reason for this phenomenon is probably due to the surface stability that is damaged by the residual gas molecules in UHV environment [17,18]. Therefore, further understanding of the influence of residual gas molecules on Cs-sensitized $In_xGa_{1-x}As$ surface is crucial for improving the quantum efficiency and lifetime of the photocathode. Although a large amount of experiments on the quantum efficiency and lifetime of NEA GaAs photocathode adsorbed with residual gases have been carried out [18,19] as well as similar theoretical research such as $Ga_{0.5}Al_{0.5}As$ (001) β_2 (2 × 4) surface [20] and Cs-activated GaN nanowire [21], the adsorption mechanism of residual gas molecules on the surface of Cs-sensitized $In_xGa_{1-x}As$ is still unclear.

Fisher et al. proposed that the composition of Indium has a significant impact on the lattice matching between $In_xGa_{1-x}As$ material and the substrate. Consequently, the lattice mismatch is minimal when the composition of Indium reaches 0.53 [22]. Besides, the photoemission performance of ternary mixed crystal $In_xGa_{1-x}As$ and binary compounds GaAs is almost the same. More prominently, previous experiments have proved that the surface of GaAs (001) β_2 (2 × 4) has the lowest work function and the best stability among all possible reconstruction surface models [23–25]. Furthermore, in our previous research, we revealed the activation mechanism of Cs/O co-adsorption on $In_{0.53}Ga_{0.47}As$ (001) β_2 (2 × 4) reconstruction surface during the formation of NEA state [26]. Defects have been proven to not only improve the electrical and optical properties of cathode materials [27], but also increase the electrocatalytic activity of carbon materials [28–30]. Therefore, in this paper, $In_{0.53}Ga_{0.47}As$ (001) β_2 (2 × 4) reconstruction surface was chosen to simulate the effect of residual gas adsorption on Cs-sensitized surface.

To this end, the first-principles calculation based on density functional theory (DFT) was selected to investigate the effect of residual gas (H_2, CH_4, CO, H_2O, CO_2) adsorption on the electronic and optical properties of Cs-sensitized surface. The noteworthy results revealed the adsorption mechanism of residual gas molecules on the $In_{0.53}Ga_{0.47}As$ (001) β_2 (2 × 4) surface, which has a far-reaching guiding significance for experimentalist to further improve the activation process in the UHV environments.

2. Calculation details and models

All calculations were based on the projector augmented wave (PAW) pseudo-potential [31] in the Vienna *ab initio* simulation package (VASP) [32,33]. The generalized gradient approximation (GGA) of Perdew-Burke-Ernzerh (PBE) was subsequently used to deal with the interaction between electrons [34]. The cut-off energy was selected as 520 eV, and the k-point mesh was set to 4 × 8 × 1. A suitable vacuum layer of 15 Å was used in the *z*-axis to avoid interaction between adjacent layers. For geometric optimization, convergence standards of the energy and force of each atom were less than 10^{-4} eV and 10^{-2} eV/Å, respectively. Fig. 1 shows the schematic diagram of the Cs-sensitized $In_{0.53}Ga_{0.47}As$ (001) β_2 (2 × 4) surface adsorbed with five different residual gas molecules, respectively. In previous studies, it was found that the best coverage of Cs atoms upon the $In_{0.53}Ga_{0.47}As$ (001) β_2 (2 × 4) surface is 0.75 ML [35]. Under this coverage, the surface work function is the lowest, and photoelectrons are more likely to escape from the Cs-sensitized surface. Therefore, in this work, the fundamental surface adsorption model with Cs coverage of 0.75 ML was taken as the research object, and then five kinds of gases (H_2, CH_4, CO, H_2O, CO_2) were attached atop the surface. Only one gas molecule was present in each model. Every model consists of seven atomic layers, where the bottom three layers were constrained and the upper four layers were relaxed, respectively. All structures were built based on the fundamental principle of lowest energy, and the optimized lattice constants were a = 15.98 Å, b = 7.99 Å, c = 28.37 Å. Besides, pseudo-hydrogen atoms were conventionally adopted at the bottom of the models to saturate dangling bonds [36]. All residual gas molecules were solely optimized, and the valence electron configurations were set as follows: In:

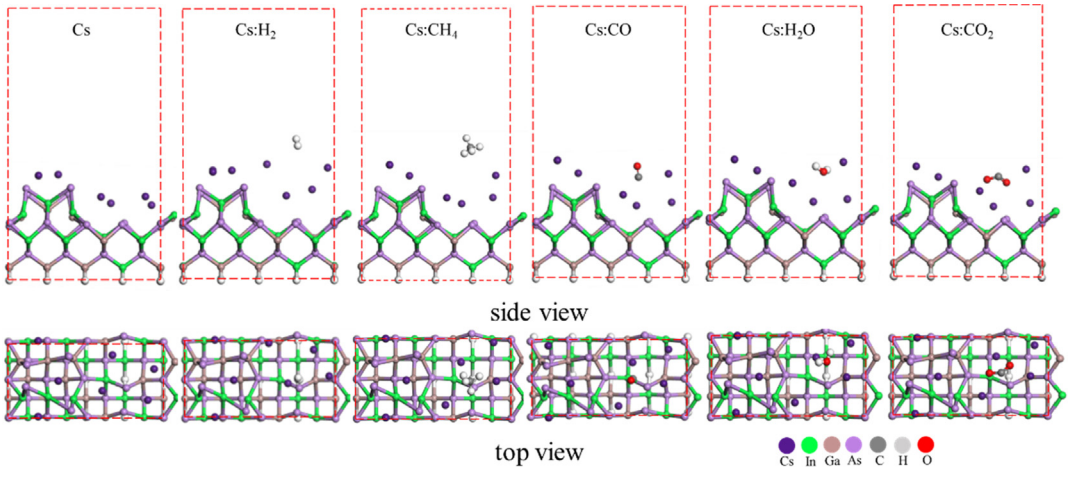

Fig. 1. The structure diagram of different residual gas molecules adsorbed on the Cs-sensitized $In_{0.53}Ga_{0.47}As$ (001) β_2 (2 × 4) surface, respectively.

$4d^{10}5s^25p^2$, Ga: $3d^{10}4s^24p^1$, As: $4s^24p^3$, Cs: $5s^25p^66s^1$, C: $2s^22p^2$, O: $2s^22p^4$, H: $1\ s^1$, respectively. Furthermore, in this paper, the unsensitized $In_{0.53}Ga_{0.47}As$ (001) β_2 (2 × 4) surface is called clean surface. In the Cs-sensitized surface models, Cs atoms are called surface Cs atoms, while in the residual gas adsorption models, Cs atoms are called inner Cs atoms, respectively.

3. Results and analysis

To determine the stability of the models and the difficulty of the residual gas adsorption, It was firstly investigated the adsorption energies of different residual gas molecules on Cs-sensitized $In_{0.53}Ga_{0.47}As$ (001) β_2 (2 × 4) surface, as shown in Fig. 2 (a). The calculation formula is set as follows [21]:

$$E_{ads} = E_{InGaAs-Cs:Gas} - E_{InGaAs-Cs} - E_{Gas} \quad (1)$$

where E_{ads} represents the adsorption energy of the model, $E_{InGaAs\text{-}Cs:Gas}$ represents the total energy of Cs and residual gas co-adsorption system, $E_{InGaAs\text{-}Cs}$ represents the energy of Cs adsorption system, and E_{Gas} represents the energy of residual gas molecule, respectively.

The calculated adsorption energies of all the models are: −0.02 eV, −0.17 eV, −0.48 eV, −0.28 eV, −1.09 eV, respectively. The negative values indicate that all adsorption models are physically stable, and the adsorption process is exothermic. The smaller the adsorption energy is, the more stable the structure, indicating that the residual gas molecules are easier to adhere to on the Cs-sensitized surface. Among the five residual gas molecules, CO_2 molecule is the most readily adsorbed on the Cs-sensitized surface, thereby affecting the stability of the surface; while CH_4 molecule is the most difficult to adsorb on the Cs-sensitized surface.

According to the 'three-step' theory [37], the photoelectrons need to overcome a certain surface barrier in order to escape from the $In_{0.53}Ga_{0.47}As$ (001) surface to the vacuum environment. Therefore, in order to have a deeper understanding of the influence of different residual gas molecules on the surface barrier, the following electronic parameters were calculated: work function (φ), electron affinity (χ), and the change of electron affinity ($\Delta\chi$). The calculation formulas of these parameters are as follows:

$$\varphi = E_{Vacuum} - E_f \quad (2)$$

$$\chi = E_{Vacuum} - E_C \quad (3)$$

$$\Delta\chi = \chi_1 - \chi_2 \quad (4)$$

where E_{Vacuum} represents the vacuum level, E_f represents the Fermi level, χ_2 represents the electron affinity of the Cs adsorption system, and χ_1 represents the electron affinity of the residual gas adsorption system, respectively.

In this perspective, the surface work function of the residual gas adsorption systems was calculated. As shown in Fig. 2(b), the work function of Cs-sensitized system is 4.02 eV. However, the adsorption of residual gas molecules results in a substantial increase in work functions, which can hinder the emission of photoelectrons. This ultimately affects the quantum efficiency of the photocathode. Specifically, among the five residual gas molecules, the adsorption of CO_2 molecule results in the largest change of work function, indicating the highest attenuation of photocathode quantum efficiency. The calculated electron affinity of the Cs-sensitized system is 3.34 eV, which is not enough to form the NEA state [35]. Moreover, it can be seen from Fig. 3(a) that the simultaneous increase in surface work function is mainly due to the upward level of the vacuum. The adsorption of residual gas molecules can further increase the electron affinity of the Cs-sensitized surface, which will seriously hinder the formation of the low-affinity surface relying on inner Cs atoms. Primarily, the electron affinity of the Cs-sensitized surface is the largest with the adsorption of CO_2 molecule, while it is the smallest with the adsorption of H_2O molecule, as shown in Fig. 3 (b). Additionally, the variation of electron affinity caused by CO_2 molecule is the most obvious. In this regard, special attention should be paid to the concentration of CO_2 gas in the vacuum environments.

In principle, the adsorption of residual gas molecules enlarges the surface work function and electron affinity, which can greatly hinder the transmission of electrons. Therefore, it was also calculated the charge transfer between the residual gas molecules and surface atoms based on the Bader charge population, as shown in Fig. 4. It can be seen from the figure that when only Cs atoms are adsorbed, surface Cs atoms firstly provide electrons to surface atoms to form a dipole moment, which creates a built-in electric field between the clean surface and surface Cs atoms. This leads to the reduction of the work function of clean surface. After the adsorption of residual gas molecules on the Cs-sensitized surface, inner Cs atoms will not only provide electrons to the surface atoms but also provide electrons to the residual gas molecules. In addition, CO_2 molecule gets the most electrons from inner Cs atoms, indicating that the ionization phenomenon of CO_2 molecule is the most obvious.

Of particular note is that two different dipole moments are generated in the residual gas adsorption system. The first is dipole 1 [Cs-$In_{0.53}Ga_{0.47}As$], which is directed from inner Cs atoms to the clean surface, and the other is dipole 2 [Cs-Gas], which is directed from inner Cs atoms to the residual gas molecules, as shown in Fig. 5. The formation of dipole 2 will induce a reverse electric field

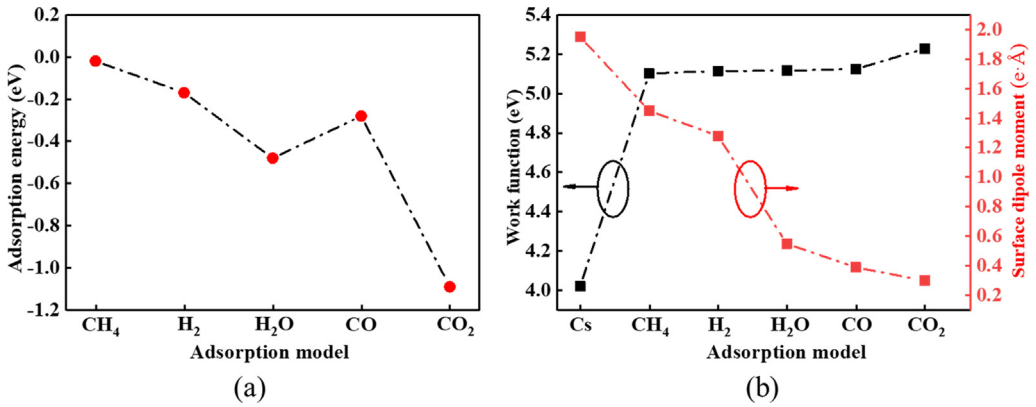

Fig. 2. The calculation results of different residual gas molecules (CH_4, H_2, H_2O, CO, CO_2) adsorbed on the Cs-sensitized $In_{0.53}Ga_{0.47}As$ (001) β_2 (2 × 4) surface; (a) adsorption energies (b) work functions and surface dipole moments (all adsorbates), respectively.

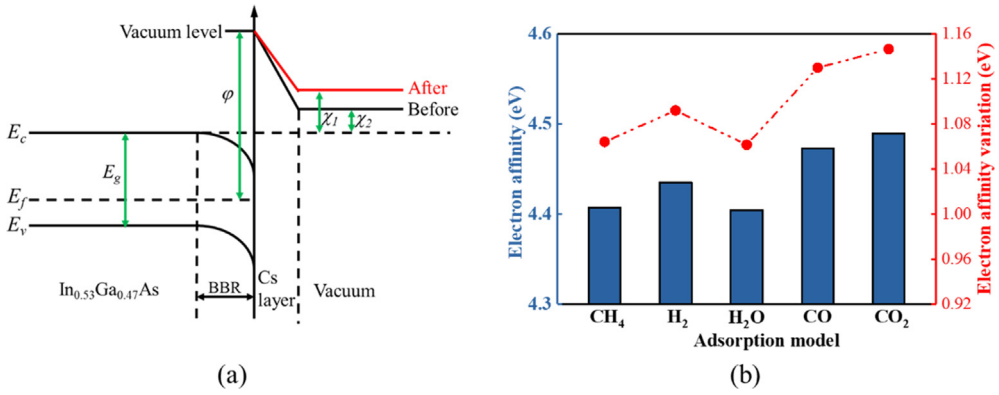

Fig. 3. (a) Schematic diagram of the surface barrier on the Cs-sensitized $In_{0.53}Ga_{0.47}As$ (001) β_2 (2 × 4) surface adsorbed with residual gas molecules; (b) The calculated electron affinity and its variation on the surface adsorbed with residual gas molecules, respectively.

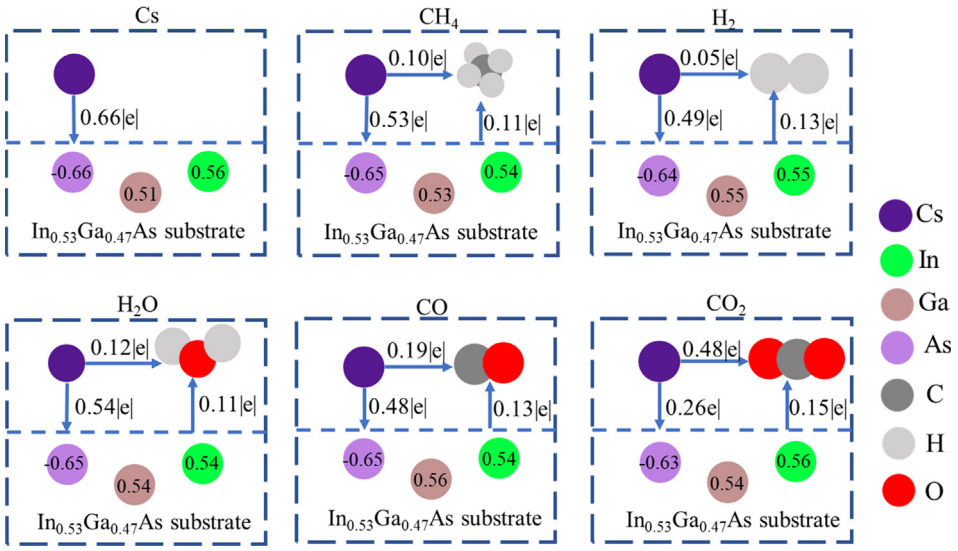

Fig. 4. Schematic diagram of charge transfer between Cs atoms, residual gas molecules and $In_{0.53}Ga_{0.47}As$ (001) surface. The blue arrow indicates the direction of electron transmission. However, the positions of the atoms in the figure do not represent the actual position in the models. (For interpretation of the references to colour in this figure legend, the reader is referred to the web version of this article.)

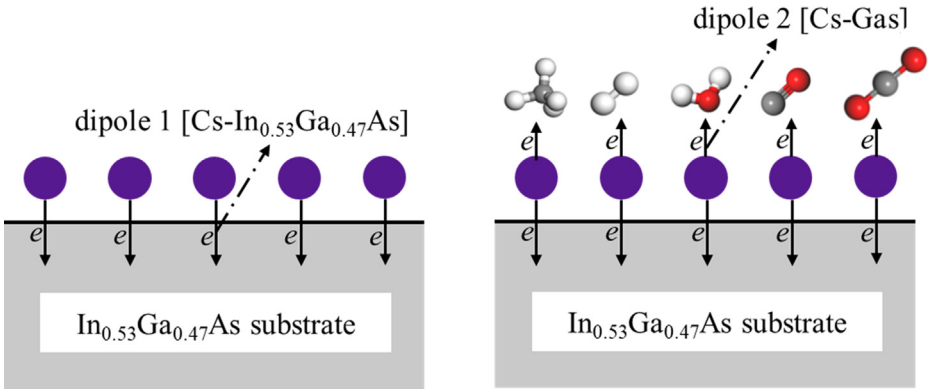

Fig. 5. Schematic diagram of the dipoles on the Cs-sensitized surface before and after the residual gas adsorption.

between the residual gas molecules and the Cs-sensitized surface, thereby increasing the surface work function. Moreover, compared with the Cs-sensitized surface, the charge transfer between the residual gas molecules and the $In_{0.53}Ga_{0.47}As$ (001) surface atoms is relatively weak, indicating that the redistribution of charge is mainly concentrated in the sensitive layer.

In parallel, to further explore the influence of residual gas molecules adsorption on surface dipoles, the dipole moments between all adsorbates and the surface were evaluated through the method proposed by Hogan et al. [38], as shown in Fig. 2(b). We also calculated the average charge Q, average dipole length d_z and dipole moment p_z of the new dipole 2 [Cs-Gas], as shown in

Fig. 6. In particular, the charge density difference $\Delta\rho(r)$ was calculated as follows [38]:

$$\Delta\rho(r) = \rho_{gas}(r) + \rho_{cs-surface}(r) - \rho_{gas/cs-surface}(r) \quad (5)$$

where $\rho_{gas}(r)$and $\rho_{cs\text{-}surface}(r)$ represent the charge density of residual gas molecules and the Cs-sensitized surface, respectively. $\rho_{gas/cs\text{-}surface}(r)$ represents the charge density of the residual gas molecules adsorbed surface. r represents the relative position of the adsorbate upon the surface. The average charge $Q^{\pm}$ and dipole length d_z between the inner Cs atoms and residual gas molecules are calculated as follows:

$$\Delta\rho(r_z) \geq 0, Q^{+} = \sum \Delta\rho(r_z); \Delta\rho(r_z) \leq 0, Q^{-} = \sum \Delta\rho(r_z) \quad (6)$$

$$Q^{\pm} = Q^{+} + Q^{-} \quad (7)$$

$$d_z = \frac{\sum \Delta\rho(r_z)z}{Q^{+}}|_{\Delta\rho(r_z>0)} - \frac{\sum \Delta\rho(r_z)z}{Q^{-}}|_{\Delta\rho(r_z<0)} \quad (8)$$

The dipole moment p_z is calculated:

$$p_z = |Q^{\pm}| \times d_z \quad (9)$$

Typically, after the adsorption of residual gas molecules on the Cs-sensitized surface, the dipole moment between adsorbates and the surface greatly reduces, as shown in Fig. 2 (b). This can further explain the increased surface work function. Moreover, the change in the surface dipole moment caused by the adsorption of CO_2 molecule is the biggest, which indicates that CO_2 molecules are more likely to damage the stability of cathode surface. The increase in surface dipole moment of different residual gas adsorption systems follows the order of $CH_4 < H_2 < H_2O < CO < CO_2$. From the calculation results of the new dipole 2 [Cs-Gas] in Fig. 6, the distance between the charge center of the inner Cs atoms and the H_2 molecule is the largest, and CO_2 molecule has the maximum negative charge owing to the stronger ionization. The adsorption of residual gas molecules not only produces electrons from inner Cs atoms and becomes negatively charged, but also makes the charge center of the adsorbates escape from the surface. The dipole moment from inner Cs atoms to CO_2 gas molecule is the largest, which weakens the interaction between the inner Cs atoms and the clean surface. Above all, it is demonstrated that CO_2 molecule greatly damaged the Cs-sensitized $In_{0.53}Ga_{0.47}As$ (001) surface.

Likewise, in order to explore the adsorption mechanism of residual gas molecules on Cs-sensitized $In_{0.53}Ga_{0.47}As$ (001) β_2 (2 × 4) surface, a detailed analysis of the band structures of different adsorption models was done, as shown in Fig. 7. Moreover, we only depict the energy band structure changes from −2 eV to 2 eV. Although the PBE method based on DFT will make the calculated band gap smaller than the theoretical, it will not affect the analysis of the electronic structure of the residual gas adsorption system [39,40]. As shown, the band gap of the Cs-sensitized system is 1.43 eV, while the adsorption of residual gas molecules will make the conduction band minimum (CBM) move to higher energy, and the valence band maximum (VBM) move slightly to lower energy. This in turn will increase the band gap. Meanwhile, the band structures of the Cs-sensitized system and the residual gas (namely CH_4, H_2O, CO, CO_2) adsorption systems exhibit indirect bandgap characteristics. In contrast, the adsorption of H_2 molecule makes the band structure represent direct bandgap characteristics. Consequently, among the five residual gas molecules, the band gap variation caused by H_2O molecule is the largest.

In semiconductors, the efficiency of photocarrier generation is fundamentally limited by the optical absorption and reflection [41]. Hence, we also analyzed the influence of the residual gas adsorption on the surface absorption coefficient and reflection coefficient, as shown in Fig. 8. The calculation formulas are as follows [42]:

$$\alpha = 2\omega k/c = 4\pi k/\lambda_0 \quad (10)$$

$$R(\omega) = \left[(n-1)^2 + k^2\right] / \left[(n+1)^2 + k^2\right] \quad (11)$$

where α represents the absorption coefficient, $R(\omega)$ represents the reflection coefficient. c represents the speed of light, λ_0 represents the wavelength. n and k represent the refractive index and extinction coefficient of the $In_{0.53}Ga_{0.47}As$ (001) surface, respectively.

As shown in Fig. 8 (a), the peak value of the absorption coefficient of Cs-sensitized surface reaches 6.361 × $10^5 cm^{-1}$, and the peak position is located at 4.633 eV. After the adsorption of the residual gas molecules, the peak value of the absorption coefficient increases significantly and moves toward higher-energy region. The increase in the absorption coefficient of different residual gas adsorption systems follows the order of $H_2 < CH_4 < H_2O < CO_2 < CO$. Besides, it can also be seen from Fig. 8 (b) that the adsorption of residual gas molecules will also lead to the peak of reflectivity moving toward higher-energy region. The calculated optical properties further demonstrate the harmful effect of residual gases upon the Cs-sensitized surface; however, the sensitive layer can still absorb photon normally.

4. Conclusions

Based on previous research studies [22–25,35], this study has revealed the physical mechanism of residual gas adsorption on Cs-sensitized $In_{0.53}Ga_{0.47}As$ (001) β_2 (2 × 4) surface. The residual gas molecules damage the stability of the cathode surface and then affect the quantum efficiency and lifetime of the cathode. This is consistent with the conclusions obtained in previous experiments

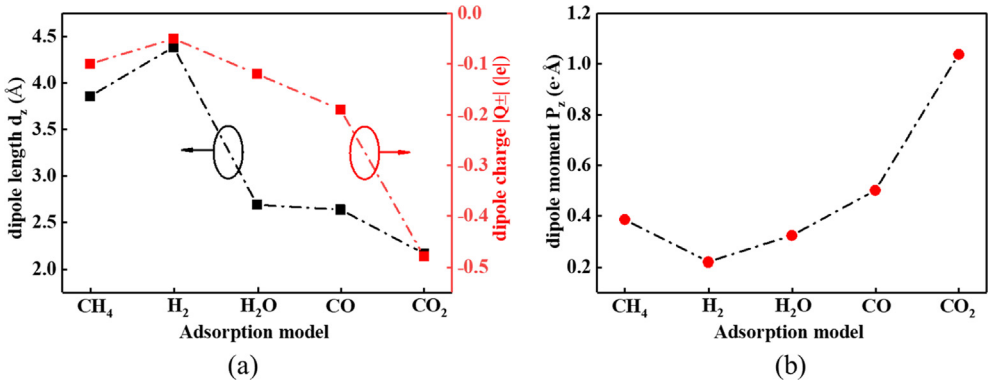

Fig. 6. Schematic diagram of the average dipole charge, dipole length and dipole moment between inner Cs atoms and residual gas molecules.

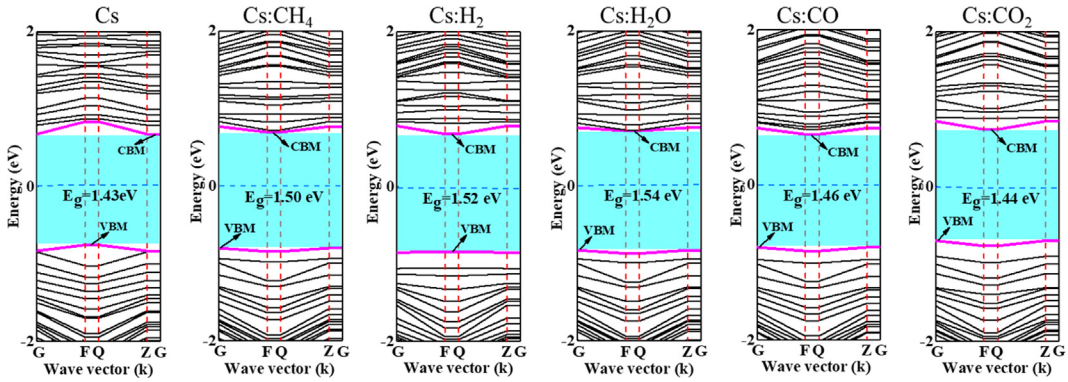

Fig. 7. The band structure diagram of different residual gas molecules adsorbed on the Cs-sensitized $In_{0.53}Ga_{0.47}As$ (001) β_2 (2 × 4) surface, respectively. The blue area represents the band gap, while the solid pink lines indicate the positions of conduction band minimum (CBM) and valence band maximum (VBM), respectively. (For interpretation of the references to colour in this figure legend, the reader is referred to the web version of this article.)

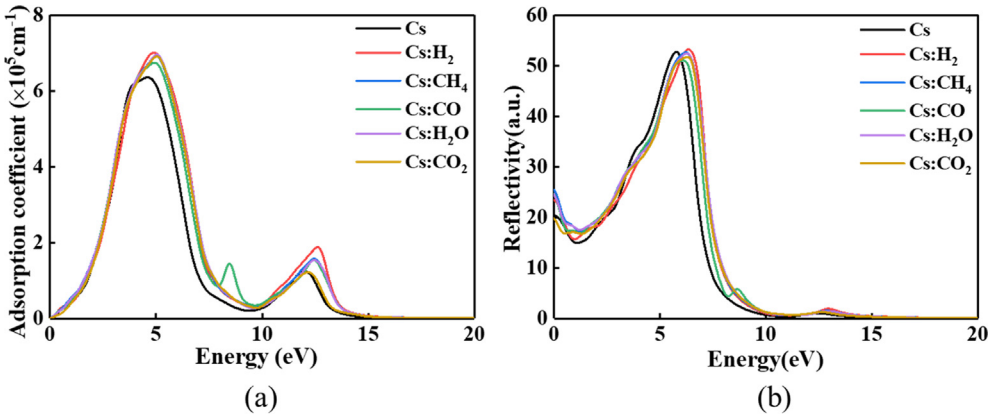

Fig. 8. Optical properties of Cs-sensitized $In_{0.53}Ga_{0.47}As$ (001) β_2 (2 × 4) surface adsorbed with different residual gas molecules (a) absorption coefficient (b) reflection coefficient, respectively.

[17,18]. What's more, the residual gas molecules will contribute to the increase of the surface work function and dipole moments, as observed in $Ga_{0.5}Al_{0.5}As$ (001) β_2 (2 × 4) surface [20] and Cs-activated GaN nanowire [21]. However, compared with the $Ga_{0.5}Al_{0.5}As$ (001) β_2 (2 × 4) surface [20], this work demonstrates that residual gas molecules affect the electron affinity of the cathode surface and then damage the sensitizing effect of Cs atoms. In parallel, compared with Cs-activated GaN nanowire [21], it can be concluded that the peak values of absorption coefficients show an opposite trend, which indicates that the effect of residual gas molecules on the optical properties of different surfaces is inconsistent. According to this work, the adsorption of residual gases will adversely affect the performance of sensitized photocathodes, especially oxidizing active gases such as CO_2. It is suggested that special attention should be paid to the concentration of CO_2 gas during the surface sensitization of $In_xGa_{1-x}As$ photocathodes.

CRediT authorship contribution statement

Qianglong Fang: Investigation, Writing - original draft. **Yang Shen:** Conceptualization, Writing - review & editing, Funding acquisition. **Shuqin Zhang:** Validation, Investigation. **Xiaodong Yang:** Software, Methodology. **Lingze Duan:** Investigation, Visualization. **Liang Chen:** Resources, Formal analysis. **Shiqing Xu:** Resources, Supervision. **Mingxia Gao:** Supervision, Project administration. **Hongge Pan:** Supervision, Project administration.

Declaration of Competing Interest

The authors declare that they have no known competing financial interests or personal relationships that could have appeared to influence the work reported in this paper.

Acknowledgement

This work was supported by the National Key Research and Development Program of China (Grant No. 2017YFF0210800), the National Natural Science Foundation of China (Grant Nos. 62004183, 61775203 and 62075205), Natural Science Foundation of Zhejiang Province (Grant Nos. LQ21F050011, LZ20F050001 and LGG19F050005) and the Fundamental Research Funds for the Provincial Universities of Zhejiang (Grant No. 2020YW48).

References

[1] M.P. Surh, S.G. Louie, M.L. Cohen, Quasiparticle energies for cubic BN, BP, and BAs, Phys. Rev. B 43 (1991) 9126–9132.
[2] G. Rehman, M. Shafiq, Saifullah, et al., Electronic band structures of the highly desirable III–V semiconductors: TB-mBJ DFT Studies, J. Electron. Mater. 45 (2016) 3314–3323.
[3] J.J. Yang, Z.Z. Liu, P. Jurczak, et al., All-MBE grown InAs/GaAs quantum dot lasers with thin Ge buffer layer on Si substrates, J. Phys. D Appl. Phys. 54 (2021) 035103.
[4] A.B.P. Mbeunmi, M. El-Gahouchi, R. Arvinte, et al., Direct growth of GaAs solar cells on Si substrate via mesoporous Si buffer, Sol. Energy Mater. Sol. Cells 217, 110641 (2020).
[5] S.S. Mohanty, U. Bhanja, G.P. Mishra, Impact of Underlap Engineering on Stepped Poly Gate $In_{0.53}Ga_{0.47}As$/InP Heterostructure Metal Oxide

Semiconductor Field Effect Transistor for Better Analog Performance, J. Nanoelectron. Optoelectron. 14 (2019) 923–931.
[6] L. Geelhaar, R.A. Bartynski, F. Ren, et al., Photoluminescence and x-ray photoelectron spectroscopy study of S-passivated InGaAs (001), J. Appl. Phys. 80 (1996) 3076–3082.
[7] Z. Liu, Y. Sun, S. Peterson, et al., Photoemission study of Cs–NF_3 activated GaAs (100) negative electron affinity photocathodes, Appl. Phys. Lett. 92 (2008) 241107.
[8] Y. Sun, R.E. Kirby, T. Maruyama, et al., The surface activation layer of GaAs negative electron affinity photocathode activated by Cs, Li, and NF_3, Appl. Phys. Lett. 95 (2009) 174109.
[9] Y. Diao, L. Lei, S.H. Xia, et al., Surface sensitization mechanism on negative electron affinity p-GaN nanowires, Superlattices Microstruct. 115 (2018) 140–153.
[10] J.J. Zou, B.K. Chang, Z. Yang, et al., Evolution of surface potential barrier for negative-electron-affinity GaAs photocathodes, J. Appl. Phys. 105 (2009) 013714.
[11] S. Karkare, D. Dimitrov, W. Schaff, et al., Monte Carlo charge transport and photoemission from negative electron affinity GaAs photocathodes, J. Appl. Phys. 113 (2013) 104904.
[12] A. Rogalski, K. Chrzanowski, Infrared devices and techniques (revision), Metrol. Measur. Syst. 21 (2014) 565–618.
[13] P. Sen, D.S. Pickard, J.E. Schneider, et al., Lifetime and reliability results for a negative electron affinity photocathode in a demountable vacuum system, J. Vac. Sci. Technol., B 16 (1998) 3380–3384.
[14] N.I. Yakovleva, A.V. Nikonov, Lifetime of Minority Charge Carriers in InGaAs-Based Structures, J. Commun. Technol. Electron. 65 (2020) 340–346.
[15] S. Pastuszka, M. Hoppe, D. Kratzmann, et al., Preparation and performance of transmission-mode GaAs photocathodes as sources for cold dc electron beams, J. Appl. Phys. 88 (2000) 6788–6800.
[16] J.J. Zou, B.K. Chang, Z. Yang, et al., Stability and photoemission characteristics for GaAs photocathodes in a demountable vacuum system, Appl. Phys. Lett. 92 (2008) 172102.
[17] N. Chanlek, J.D. Herbert, R.M. Jones, et al., The degradation of quantum efficiency in negative electron affinity GaAs photocathodes under gas exposure, J. Phys. D Appl. Phys. 47 (2014) 055110.
[18] N. Chanlek, J.D. Herbert, R.M. Jones, et al., High stability of negative electron affinity gallium arsenide photocathodes activated with Cs and NF_3, J. Phys. D Appl. Phys. 48 (2015) 375102.
[19] T. Wada, T. Nitta, T. Nomura, et al., Influence of Exposure to CO, CO_2 and H_2O on the Stability of GaAs Photocathodes, Jpn. J. Appl. Phys. 29 (1990) 2087–2091.
[20] X.H. Yu, Y.J. Du, B.K.Chang, et al., The adsorption of Cs and residual gases on Ga0.5Al0.5As (001) β2 (2×4) surface: A first principles research, Appl. Surf. Sci. 290 (2014) 142–147.
[21] F.F. Lu, L. Liu, J. Tian, Residual gas adsorption effect on the stability of Cs-activated GaN nanowire photocathode, Appl. Surf. Sci. 497 (2019) 143791.
[22] D.G. Fisher, R.E. Enstrom, J.S. Escher, et al., Photoelectron surface escape probability of (Ga, In) As : Cs-O in the 0.9 to 1.6 um range, J. Appl. Phys. 43 (1972) 3815–3823.
[23] T. Hashizume, Q.K. Xue, J. Zhou, et al., Structures of As-Rich GaAs (001)-(2×4) Reconstructions, Phys. Rev. Lett. 73 (1994) 2208–2211.
[24] T. Hashizume, Q.K. Xue, A. Ichimiya, et al., Determination of the surface structures of the GaAs (001)-(2×4) As-rich phase, Phys. Rev. B 51 (1995) 4200–4212.
[25] W.G. Schmidt, F. Bechstedt, Geometry and electronic structure of GaAs (001) (2×4) reconstructions, Phys. Rev. B 54 (1996) 16742–16748.
[26] L. Chen, Y. Shen, X.D. Yang, et al., Research on Cs/O activation process of near-infrared $In_{0.53}Ga_{0.47}As$ photocathodes, J. Alloy. Compd. 831 (2020) 154869.
[27] L. Liu, Y. Diao, S.H. Xia, Intrinsic point defects in pristine and Zn-doped GaAs nanowire surfaces: A first-principles investigation, Appl. Surf. Sci. 514 (2020) 145906.
[28] L.Z. Zhang, Y. Jia, G.P. Gao, et al., Graphene Defects Trap Atomic Ni Species for Hydrogen and Oxygen Evolution Reactions, Chem 4 (2018) 285–297.
[29] Y. Jia, K. Jiang, H.T. Wang, et al., The Role of Defect Sites in Nanomaterials for Electrocatalytic Energy Conversion, Chem 5 (2019) 1371–1397.
[30] X.C. Yan, Y. Jia, X.D. Yao, Defects on carbons for electrocatalytic oxygen reduction, Chem. Soc. Rev. 47 (2018) 7628–7658.
[31] G. Kresse, D. Joubert, From ultrasoft pseudopotentials to the projector augmented-wave method, Phys. Rev. B 59 (1999) 1758–1775.
[32] P.E. Blöchl, Projector augmented-wave method, Phys. Rev. B 50 (1994) 17953–17979.
[33] G. Kresse, J. Furthmüller, Efficient iterative schemes for ab initio total-energy calculations using a plane-wave basis set, Phys. Rev. B 54 (1996) 11169–11186.
[34] M.C. Payne, M.P. Teter, D.C. Allan, et al., Iterative minimization techniques for ab initio total-energy calculations: molecular dynamics and conjugate gradients, Rev. Mod. Phys. 64 (1992) 1045–1097.
[35] Y. Shen, X.D. Yang, Y. Bian, et al., Early stage of Cs activation mechanism for In0.53Ga0.47As (001) β2 (2×4) surfaces: Insights from first-principles calculations, Appl. Surf. Sci., 457 (2018) 150–155.
[36] S. Krukowski, P. Kempisty, P. Strak, Electrostatic condition for the termination of the opposite face of the slab in density functional theory simulations of semiconductor surfaces, J. Appl. Phys. 105 (2009) 113701.
[37] W.E. Spicer, A. Herrera-Gomez, Modern theory and applications of photocathodes, Proc. SPIE 2022 (1993) 18–33.
[38] C. Hogan, D. Paget, Y. Garreau, et al., Early stages of cesium adsorption on the As-rich c(2×8) reconstruction of GaAs (001): Adsorption sites and Cs-induced chemical bonds, Phys. Rev. B 68 (2003) 205313.
[39] A.J. Garza, G.E. Scuseria, Predicting Band Gaps with Hybrid Density Functionals, J. Phys. Chem. Lett. 7 (2016) 4165–4170.
[40] N.N. Fu, E.L. Li, Z. Cui, et al., The electronic properties of phosphorus-doped GaN nanowires from first-principle calculations, J. Alloy. Compd. 596 (2014) 92–97.
[41] D. Jariwala, T.J. Marks, M.C. Hersam, Mixed-dimensional van der Waals heterostructures, Nat. Mater. 16 (2017) 170–181.
[42] J.P. Long, L.J. Yang, D.M. Li, et al., First-principles calculations of structural, electronic, optical and elastic properties of $LiEu_2Si_3$, Solid State Sci. 20 (2013) 36–39.